Neurotherapeutics (2018) 15:1112–1126
https://doi.org/10.1007/s13311-018-0657-9

ORIGINAL ARTICLE

Early Treatment with Quinidine in 2 Patients with Epilepsy of Infancy with Migrating Focal Seizures (EIMFS) Due to Gain-of-Function *KCNT1* Mutations: Functional Studies, Clinical Responses, and Critical Issues for Personalized Therapy

Robertino Dilena[1] · Jacopo C. DiFrancesco[2,3] · Maria Virginia Soldovieri[4] · Antonella Giacobbe[1] · Paolo Ambrosino[4] · Ilaria Mosca[4] · Maria Albina Galli[1] · Sophie Guez[1] · Monica Fumagalli[1] · Francesco Miceli[5] · Dario Cattaneo[6] · Francesca Darra[7] · Elena Gennaro[8] · Federico Zara[8] · Pasquale Striano[9] · Barbara Castellotti[10] · Cinzia Gellera[10] · Costanza Varesio[11] · Pierangelo Veggiotti[12] · Maurizio Taglialatela[4,5,13]

Published online: 15 August 2018

Abstract

Epilepsy of infancy with migrating focal seizures (EIMFS) is a rare early-onset developmental epileptic encephalopathy resistant to anti-epileptic drugs. The most common cause for EIMFS is a gain-of-function mutation in the *KCNT1* potassium channel gene, and treatment with the KCNT1 blocker quinidine has been suggested as a rational approach for seizure control in EIMFS patients. However, variable results on the clinical efficacy of quinidine have been reported. In the present study, we provide a detailed description of the clinical, genetic, *in vitro*, and *in vivo* electrophysiological profile and pharmacological responses to quinidine of 2 EIMFS unrelated patients with a heterozygous *de novo KCNT1* mutation: c.2849G>A (p.R950Q) in patient 1 and c.2677G>A (p.E893K) in patient 2. When expressed heterologously in CHO cells, KCNT1 channels carrying each variant showed gain-of-function effects, and were more effectively blocked by quinidine when compared to wild-type KCNT1 channels. On the basis of these *in vitro* results, add-on quinidine treatment was started at 3 and 16 months of age in patients 1 and 2, respectively. The

Robertino Dilena, Jacopo C. DiFrancesco and Maria Virginia Soldovieri contributed equally to this work.

Electronic supplementary material The online version of this article (https://doi.org/10.1007/s13311-018-0657-9) contains supplementary material, which is available to authorized users.

✉ Maurizio Taglialatela
mtaglial@unina.it

[1] Pediatric Epileptology and Neurophysiology (RD), Infantile Neuropsichiatry (AG), Cardiology (MAG), High Intensity Pediatric Care (SG), Neonatology (MF), Fondazione IRCCS Ca' Granda Ospedale Maggiore Policlinico, 20122, Milan, Italy

[2] Clinical Neurophysiology and Epilepsy Center, Fondazione IRCCS Istituto Neurologico Carlo Besta, 20133, Milan, Italy

[3] Department of Neurology, San Gerardo Hospital, School of Medicine and Surgery, Milan Center for Neuroscience (NeuroMi), University of Milano-Bicocca, 20900, Monza, Italy

[4] Department of Medicine and Health Science, University of Molise, 86100, Campobasso, Italy

[5] Division of Pharmacology, Department of Neuroscience, University of Naples "Federico II", 80131, Naples, Italy

[6] Unit of Clinical Pharmacology, ASST Fatebenefratelli Sacco, 20157, Milan, Italy

[7] Department of Surgical, Odontostomatological, and Maternal-Infantile Sciences, University of Verona, 37134, Verona, Italy

[8] Laboratory of Genetics, E.O. Ospedali Galliera, 16128, Genoa, Italy

[9] Pediatric Neurology and Muscular Diseases Unit, Department of Neurosciences, Rehabilitation, Ophthalmology, Genetics, Maternal and Child Health, University of Genoa, "G. Gaslini" Institute, 16147, Genoa, Italy

[10] Unit of Genetics of Neurodegenerative and Metabolic Diseases, Fondazione IRCCS Istituto Neurologico Carlo Besta, 20133, Milan, Italy

[11] Department of Child Neurology and Psychiatry, "C. Mondino" National Neurological Institute, 27100, Pavia, Italy

[12] Department of Biomedical and Clinical Sciences, Children's Hospital Vittore Buzzi, University of Milan, and Pediatric Neurology, 20154, Milan, Italy

[13] Department of Neuroscience, University of Naples "Federico II", Via Pansini 5, 80131 Naples, Italy

results obtained reveal that quinidine significantly reduced seizure burden (by about 90%) and improved quality of life in both patients, but failed to normalize developmental milestones, which persisted as severely delayed. Based on the present experience, early quinidine intervention associated with heart monitoring and control of blood levels is among the critical factors for therapy effectiveness in EIMFS patients with KCNT1 gain-of-function mutations. Multicenter studies are needed to establish a consensus protocol for patient recruitment, quinidine treatment modalities, and outcome evaluation, to optimize clinical efficacy and reduce risks as well as variability associated to quinidine use in such severe developmental encephalopathy.

Key Words: KCNT1 · Developmental encephalopathy · Epilepsy of infancy with migrating focal seizures (EIMFS) · Quinidine · Therapeutic drug monitoring (TDM)

INTRODUCTION

Epilepsy of infancy with migrating focal seizures (EIMFS or malignant migrating partial seizures of infancy, MMPSI) is a rare devastating early-onset developmental epileptic encephalopathy characterized by refractory focal seizures migrating from one brain region or hemisphere to the other with polymorphic ictal semeiology. Seizures are associated with autonomic features, developmental arrest or regression, severe disability, and high probability of death in the first years of life [1]. Although mutations in several genes, including *SCN1A*, *PLCB1*, *SLC25A22*, and *TBC1D24*, have been associated with EIMFS [2], up to 50% of patients carry *de novo* heterozygous mutations in the *KCNT1* gene [3]. Notably, *KCNT1* mutations have been also found in patients affected with autosomal-dominant or sporadic nocturnal frontal lobe epilepsy [4], Ohtahara syndrome [5], multifocal epilepsy, and West [6, 7] and Brugada [8] syndromes. More recently, the phenotypic spectrum of epilepsy syndromes associated to *KCNT1* mutations has been further expanded, including mesial temporal lobe epilepsy, cerebellar ataxia, and intellectual disability [9, 10].

The *KCNT1* gene encodes for potassium (K^+) channel subunits (also called Slack, Slo2.2 or KCa4.1) having a topological arrangement similar to that of classical voltage-gated K_v channel subunits, with 6 transmembrane segments (S_1-S_6), and a pore-lining loop between S_5 and S_6 [11]; KCNT1 subunits assemble as homo- or hetero-tetramers with highly homologous KCNT2 (also called Slick or Slo2.1) subunits to form functional channels [12]. KCNT1 and KCNT2 subunits provide a major contribution to Na^+-dependent K^+ currents (IK_{Na}), a primary mechanism for protection against ischemia in cardiomyocytes and neurons [11]. In intrinsically bursting neocortical neurons, IK_{Na} is involved in activity-dependent afterhyperpolarization (AHP) and in the maintenance of rhythmic burst recurrence during sustained depolarization [13]. Moreover, KCNT1 channels also provide a major contribution to IK_{Na} in small diameter DRG neurons [14], and regulate synaptic transmission within the spinal cord dorsal horn [15], thus playing a prominent role in nociception.

In vitro functional studies have shown that KCNT1 subunits carrying EIMFS-causing variants generate larger currents when compared to wild-type KCNT1 channels, leading to the concept that a gain-of-function mechanism is responsible for epileptogenesis associated with *KCNT1* mutations [3]. Based on the ability of KCNT1 blockers like quinidine and bepridil to inhibit KCNT1 mutant channels [16, 17], targeted therapy with quinidine has been undertaken in EIMFS patients, resulting in variable anti-convulsant efficacy ranging from dramatic positive responses [18–20] to a lack of efficacy or excessive toxicity [21–23]. Despite the relevance of these therapeutic attempts for personalized therapy in patients with *KCNT1*-related epilepsies, several clinical issues remain to be settled before shared protocols for quinidine treatment can be rigorously implemented.

Here, we present the clinical, genetic, *in vitro*, and *in vivo* electrophysiological profile and pharmacological responses to quinidine of 2 unrelated EIMFS patients each carrying a heterozygous *de novo KCNT1* mutation. The results obtained reveal that both mutations cause strong, quinidine-sensitive gain-of-function effects on KCNT1 currents *in vitro*; notably, in agreement with these *in vitro* results, clinical use of quinidine significantly reduced seizure burden and improved quality of life in both patients, but failed to normalize developmental milestones, which persisted as severely delayed. Based on these results and on a critical review of the available cases described in the literature, we also attempt to highlight the critical issues (such as timing of intervention, cardiac monitoring, therapeutic drug monitoring, among others) which, in our experience, need to be optimized to maximize treatment efficacy and reduce risks and variability associated with quinidine use in such devastating developmental epilepsy.

MATERIAL AND METHODS

DNA extraction and genetic screening

After signed informed consent, blood samples were obtained from patients and relatives for genetic analyses. Genomic DNA was prepared from peripheral-blood leukocytes using standard procedures (QIAsymphony S, Qiagen, Hilden, Germany), according to the manufacturer's instructions. The genetic screening was performed in 2 different centers

(Gaslini Institute in Genoa for patient 1, Neurological Institute C. Besta in Milan for patient 2), using next-generation sequencing (NGS) methods with a MiSeq sequencer (Illumina Inc., San Diego, CA, USA) for the analysis of genes involved in the pathogenesis of epileptic encephalopathies. The genes analyzed in each of the 2 panels are reported in Supplementary Fig. 1. Data analysis was performed using the following softwares: Illumina MiSeq Reporter vs 2.4.60, Illumina Variant Studio vs 2.2, Qiagen CLC Genomics Workbench vs 7.0. Variants with MAF > 1% reported in the dbSNP (https://www.ncbi.nlm.nih.gov/projects/SNP), 1000 Genome (browser.1000genomes.org), EVS database (evs.gs.washington.edu), ExAC database (http://exac.broadinstitute.org/), and GnomAD browser (http://gnomad.broadinstitute.org) were considered benign and excluded from the report. Sanger sequencing on ABI 3130/3730 was added for the regions not well covered (coverage < 20X) to ensure that coverage of each gene was more than 95%; moreover, all the true-positive calls (nucleotide variants) identified were also confirmed by Sanger sequencing.

Mutagenesis and heterologous expression of wild-type and mutant subunits

The 2 mutations investigated in the present study were engineered in a plasmid containing the cDNA for a myc-DDK-tagged human isoform 2 (Q5JUK3-2) of KCNT1 (RC214820; Origene, Rockville, MD, USA) by quick-change mutagenesis, as previously described [17]. Mutant vectors were verified by Sanger sequencing. Wild-type and mutant cDNAs were expressed in Chinese hamster ovary (CHO) cells by transient transfection using Lipofectamine 2000 (Invitrogen,

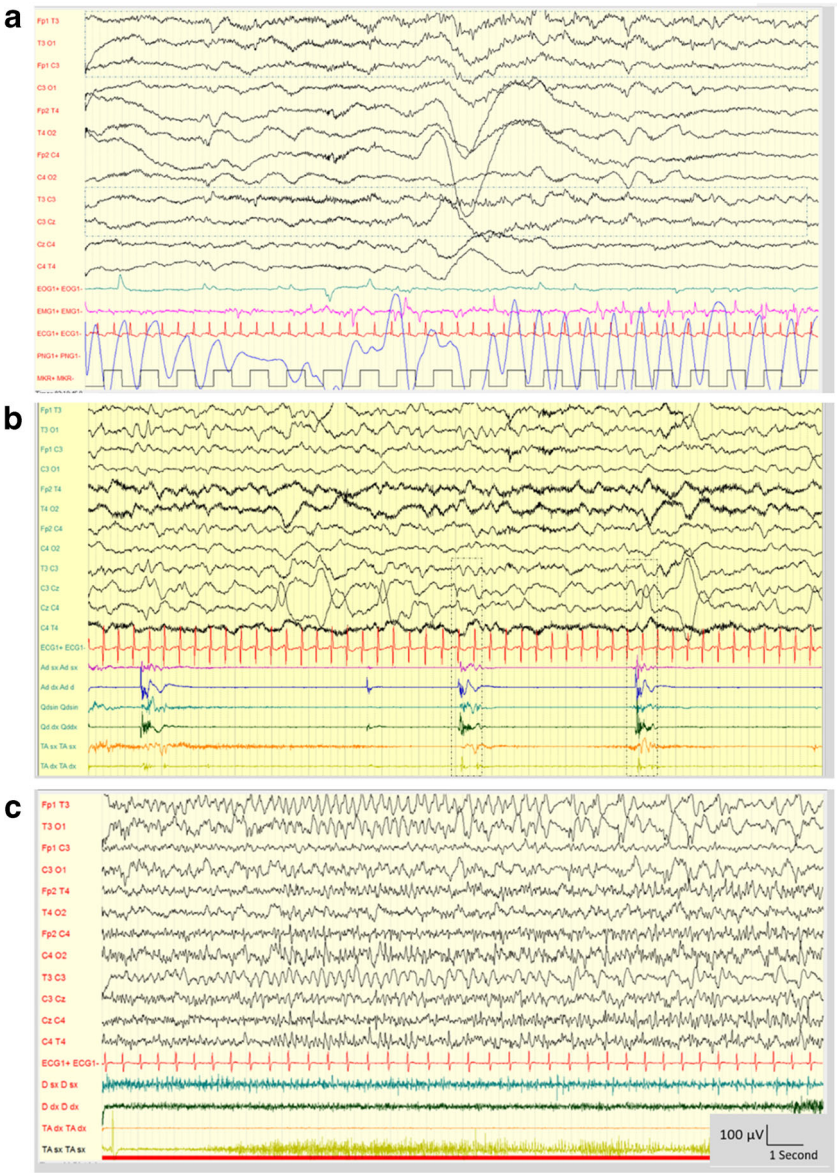

Fig. 1 Evolution of the EEG pattern during the first 3 months in patient 1. (**a**) The first seizure recorded at 2 days of life. Ictal activity is characterized by low-amplitude alpha rhythmical activity and small spikes in the left centrotemporal areas (especially T3 and C3 leads). (**b**) EEG with muscle polygraphy performed at 2 months, showing focal myoclonus at the lower limbs related to small central spikes. (**c**) EEG with muscle polygraphy at 3 months: independent epileptiform discharges of different frequency, morphology, and amplitude are seen in the two hemispheres as described for migrating focal seizures of infancy, with ictal theta activity in the left temporal channels and initial ictal faster activity in the alpha range in the right hemisphere channels; these ictal activities are associated with motor manifestations (see muscle polygraphy).

Milan, Italy), as described [24]. A plasmid encoding for the enhanced green fluorescent protein (EGFP; Clontech, Palo Alto, CA) was used as a transfection marker. Total cDNA in the transfection mixture was kept constant at 4 μg.

Whole-cell electrophysiology

Electrophysiological experiments were performed as previously described [17]. Briefly, macroscopic currents from transiently transfected CHO cells were recorded at room temperature (20-22 °C) 24 h after transfection, with an Axopatch 200B amplifier (Molecular Devices, Union City, CA) using the whole-cell configuration of the patch-clamp technique. The pipette (intracellular) solution contained (in mM): 130 KCl, 10 NaCl, 10 HEPES, 5 EGTA, 5 Mg-ATP, pH 7.3 to 7.4 with HCl; when NaCl was omitted from the pipette, KCl concentration was increased accordingly. Extracellular solution composition, as well as data acquisition and analysis, was performed as described [25]. Current densities (expressed in pA/pF) were calculated as peak K^+ currents at all tested membrane potentials divided by cell capacitance (C). Quinidine (Sigma-Aldrich, Milan, Italy) was dissolved in chloroform (final vehicle concentration ≤0.05%). In each experiment, the same volume of vehicle used to dissolve each drug to be tested was added to the control solution. Different concentrations of the drug were perfused (each cell was exposed to only 1 drug concentration, to avoid cumulative block) using a fast solution exchange system [24].

Molecular modeling Closed (PDB 5U76) and open (PDB 5U70) configurations of chicken KCNT1 [26] served as templates for homology models of human KCNT1, using the SWISS-MODEL software [27]. The models were analyzed by using Discovery Studio 4.0 Client software (BIOVIA, San Diego, CA, USA), as described [28].

Statistics Data are expressed as mean ± SEM. Statistically significant differences were evaluated with the Student *t* test or with ANOVA followed by the Student-Newman-Keul's test, with the threshold set at $p < 0.05$.

RESULTS

Clinical description of cases

Patient 1

This 12-month-old boy was born at term by unrelated healthy parents after an uneventful pregnancy and delivery. Family history was unremarkable, except for uncertain neonatal seizures in the maternal grandfather. At 2 days of life, the patient presented with daily episodes of apnea and cyanosis. EEG monitoring revealed ictal left centrotemporal alpha-theta activity suggesting the epileptic origin of the episodes (Fig. 1a). Interictal EEG showed focal spikes mainly over the bilateral centrotemporal regions. General physical and neurological examination, brain MRI, and laboratory and metabolic investigations were unremarkable. The patient was discharged from the hospital in good conditions with phenobarbital (PB; 5 mg/kg per day), initially with good seizure control. At 2 months of age, still during treatment with PB at low doses (3 mg/kg per day), parents reported the occurrence of multiple daily focal lower limb jerks in short clusters during wake and sleep. The neurological examination showed mild hypotonia, with preserved eye contact. PB was then increased to 8 mg/kg with transient benefit. A video-polygraphic-EEG documented the recurrence of bilateral lower limb myoclonias related to small spikes on the central regions (Fig. 1b), brief spasms, and bilateral clonic seizures. Oral pyridoxine (30 mg/kg for 5 days) was tried, but seizures continue to occur and carbamazepine (CBZ) was added to PB. After few days, seizures turned to more classical malignant migrating focal seizures alternating from one hemisphere to the other, with polymorphic semiology (Fig. 1c), going from no clinical manifestations to motor tonic-clonic seizures, variably combined with oral automatism, eye deviation, awareness impairment, and apneas, according to the side, distribution, and amplitude of the ictal discharge. Carbamazepine was replaced by levetiracetam (LEV) up to 60 mg/kg daily, with no effect. Therefore, based on the results of genetic and *in vitro* studies (see below), quinidine treatment was started at the dose of 2 mg/kg 4 times a day, increased every 2 to 4 days of 4 to 5 mg/kg (target 60 mg/kg) (Fig. 2). An initial response was obtained, in the first days, followed by relapse with around 100 seizures per day, so oral clonazepam up to 0.2 mg/kg and then midazolam infusion up to 0.2 mg/kg/h were added with limited seizure control. Initially, quinidine blood levels were low (between 0.2 and 1 mg/L). Suspecting a pharmacokinetic interaction, PB was gradually withdrawn and ketogenic diet was started [23]; however, no clinical benefit was observed. In the meantime, quinidine continued to be gradually titrated and when quinidine blood levels approached 2 mg/L, seizure frequency decreased. However, due to an increase in the QT interval (485 ms, Fig. 2b, marked by *), quinidine was reduced to 50 mg/kg daily. In the following days, status epilepticus occurred (200 seizures per day). Midazolam was ineffective as were LEV (up to 100 mg/kg/day), topiramate (5 mg/kg/day), and potassium bromide (up to 45 mg/kg/day). The QT interval recovered to 460 ms, and quinidine dosing was increased from 50 to 70 mg/kg in 2 weeks, and a significant reduction of seizures was finally seen. Unfortunately, the QT interval increased again to 500 ms, together with ECG signs of atrio-ventricolar block, so quinidine dose was halved with a following relapse of a high number of seizures and reduction of QT interval to 440 ms. Given the positive response to quinidine

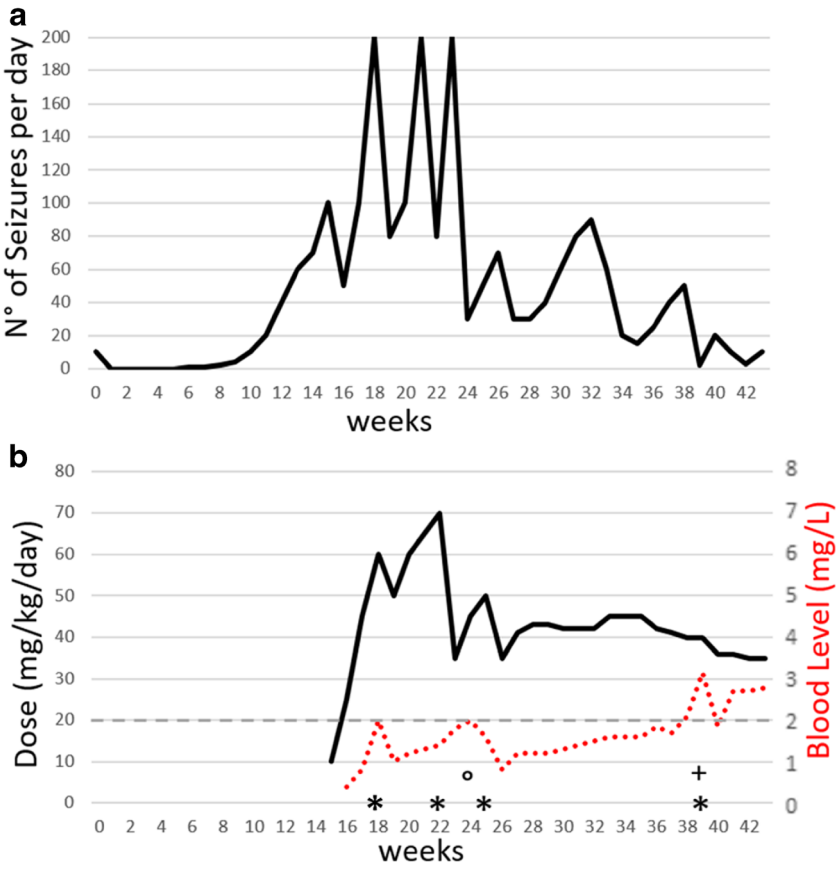

Fig. 2 Time-course of seizure activity, quinidine dosing, and blood levels during the first 10 months of life of patient 1. (**a**) Seizure number as a function of time. (**b**) Quinidine dosing (in mg/kg/day; black line) and plasma levels (in mg/L; dotted red line) in patient 1. Asterisks indicate QT > 480 ms, a degree sign indicates topiramate withdrawal, and a plus sign indicates reduction of blood ketones from around 3 to around 1.5 mmol/L in correspondence to the ketogenic diet withdrawal.

observed after refractory status epilepticus, quinidine was slowly titrated up to a target dose of 50 mg/kg/day; topiramate was simultaneously withdrawn (Fig. 2b, marked by °). After few days, another QT increase of 500 ms was observed, and the quinidine dose was reduced again to 35 mg/kg/day, leading again to QT normalization. In the following weeks, seizures increased to around 90/day and quinidine blood levels were around 1.5 mg/L; therefore, quinidine dose was increased to 45 mg/kg, with a positive effect on seizure frequency. When the ketogenic diet, considered ineffective, was withdrawn at 8 months, a new transient increase in QT (505 ms) occurred just after blood ketones dropped from around 3 to 1.5 mmol/L (Fig. 2b, marked by +), without any cardiac symptomatic complication and with quinidine blood level increased to 3 mg/L. Seizures dropped to a minimum of 2 to 20 per day, and quinidine dose was cautiously reduced to 35 mg/kg. Currently, the infant is on quinidine (45 mg/kg daily divided in 4 doses) as main therapy, together with LEV 45 mg/kg daily (LEV blood levels, 10.5 mg/L—range 10 to 40 mg). The boy has developed a severe delay of motor and cognitive milestones, poor interaction, and tetraparesis and acquired microcephaly and has currently a range of 2 to 30 seizures per day. Compared to the pre-quinidine disorganized EEG pattern with abundant multifocal slow waves and spikes and poor differentiation between sleep and awake patterns, the EEG background activity during treatment with quinidine at the current age of 1 year shows a good differentiation between sleep and awake patterns, although diffuse slow waves and multifocal sharp waves are still present (Fig. 3).

Patient 2

This 24-month-old boy was born at term from a physiological pregnancy by nonconsanguineous parents, with eutocic delivery. Family history was unremarkable. Five hours after birth, the patient experienced episodes of diffuse cyanosis, desaturation, and hyporeactivity, occasionally associated with lower-limb clonic movements. His EEG showed interhemispheric asynchrony, right central and left temporal slow waves, and sharp spikes and waves. Follow-up EEGs showed a poorly organized and asynchronous background activity with multifocal paroxysms and tendency to a burst-suppression pattern (Fig. 4a). During hospitalization in neonatal intensive care, the patient received treatments with phenobarbital, phenytoin, carbamazepine, pyridoxine, and levetiracetam, all with poor responses. Seizure frequency gradually increased up to 30 episodes per day, characterized by head and gaze deviation (right>left), winking, and oral automatisms, sometimes associated with asymmetric upper limb flexor hypertonia (right>left). At 4 months, he developed epileptic spasms with a hypsarythmic pattern. Vigabatrin, ACTH, valproic acid, nitrazepam, ketogenic diet, lamotrigine, and clonazepam in various combinations were

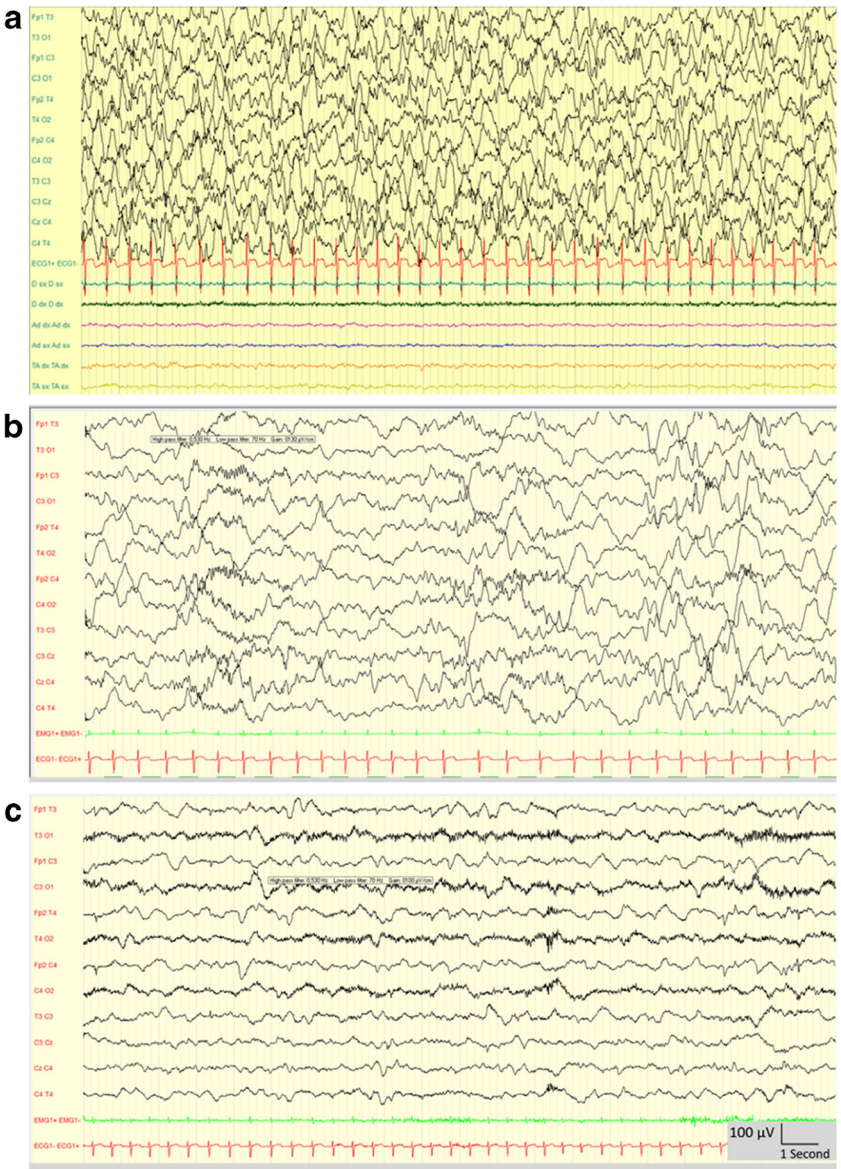

Fig. 3 EEG pattern in patient 1 before and after quinidine treatment. (**a**) EEG traces recorded at 3 months of life, showing the disorganized electrical background activity, with highly recurrent paroxysmal activity and slow activity. (**b**) NREM sleep EEG recorded at 12 months of age during quinidine treatment (blood level 3.5 mg/L); physiological sleep spindles in the central leads; some spikes in frontal and central leads. (**c**) Awake EEG recorded at 12 months of age during quinidine treatment (blood level 3.5 mg/L). Activity in the theta-delta range (slower waves than expected for age) and muscle artifacts.

tried, with lack of efficacy in the long-term period. Cannabidiol (15 mg/kg/day) was then added, but with no effect on seizures and EEG pattern (Fig. 4b). At 9 months of age, he presented clinical and EEG characteristics of EIMFS. According to the genetic results and to preclinical data (see below), therapy with quinidine was started at the age of 16 months and very slowly titrated up to 700 mg/die (58 mg/kg daily) divided in 4 doses per day, without any significant side effect. QTc remained stable between 420 and 470 msec; at last measurement performed on April 2018, QTc was 434 msec. After introduction of quinidine, a very significant reduction of seizures number was observed (> 85%). The patient is now on quinidine (58 mg/kg/day divided in 4 doses) monotherapy from 6 months. Psychomotor development is seriously impaired: at the age of 24 months, the child controls the head but does not sit unsupported. His EEG is improved, showing extremely rare interictal paroxysms, with poor organization on awake and during sleep (Fig. 4c).

Genetic findings

Genetic analysis showed a heterozygous nucleotide variant in the *KCNT1* gene (NM_020822; NP_065873): c.2849G>A in exon 24 for patient 1 and c.2677G>A in exon 23 for patient 2. Both variants were not present in the EVS, 1000 Genomes, dbSNP, and ExAC databases and occurred *de novo*, being absent in each of the parents. The c.2849G>A substitution in patient 1 is predicted to cause the *KCNT1* missense variations p.R950Q, whereas the c.2677G>A causes the p.E893K missense mutation in patient 2. Whereas the R950Q variant has been previously described in *KCNT1*-related epilepsy patients

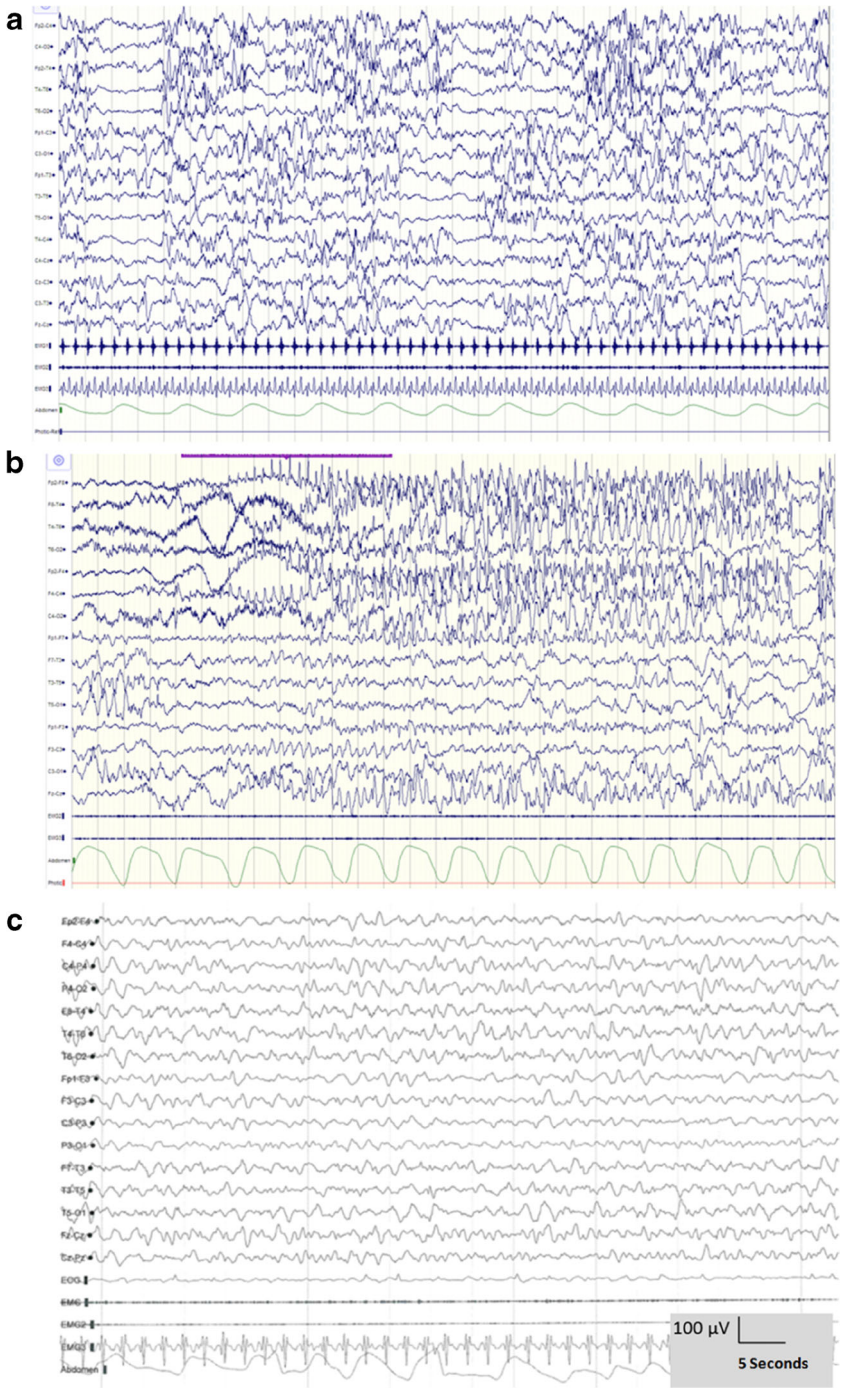

Fig. 4 EEG pattern in patient 2 before and after quinidine treatment. (**a**) Polygraphic EEG registration (EKG, breath, and deltoids) at 2 months, showing asynchronous suppression burst pattern, phases of hypo-voltage lasting at least few seconds, alternating with bursts of theta activity mixed with multifocal, bilateral, asynchronous epileptic discharges. (**b**) EEG recorded at 6 months showing theta rythmic activity on frontocentral right regions, with minimal clinical correlate. Both (**a**) and (**b**) were obtained before quinidine treatment. (**c**) Polygraphic traces recorded following quinidine treatment, showing global improvement of EEG pattern, even with persistence of a poor organized background activity with theta prevalence, but without seizures.

[6, 29–31], the E893K variant found in patient 2 is novel. Both the R950 and E893 residues are located in the regulator of K^+ conductance-2 (RCK2) domain [31] (Fig. 5a), an intracellular region in which Na^+ ions bind and regulate channel opening [11, 32]. Within RCK2, the E893 residue is positioned in the nicotinamide adenine dinucleotide (NAD^+)-binding pocket; NAD^+ binding to RCK2 increases IK_{Na} sensitivity to $[Na^+]_i$, thereby allowing current regulation by physiologically relevant changes in $[Na^+]_i$ [33]. Notably, both mutations affected residues evolutionarily conserved among different species (Fig. 5b), and were predicted to be pathogenic by SIFT (http://sift.jcvi.org/) and PolyPhen (http://genetics.bwh.harvard.edu/pph2/).

Functional characterization of homomeric wild-type and mutant KCNT1 channels

To investigate the functional properties of KCNT1 channels incorporating the 2 mutations herein reported, electrophysiological analysis was performed in CHO cells expressing wild-type or mutant KCNT1 subunits. Whereas no significant

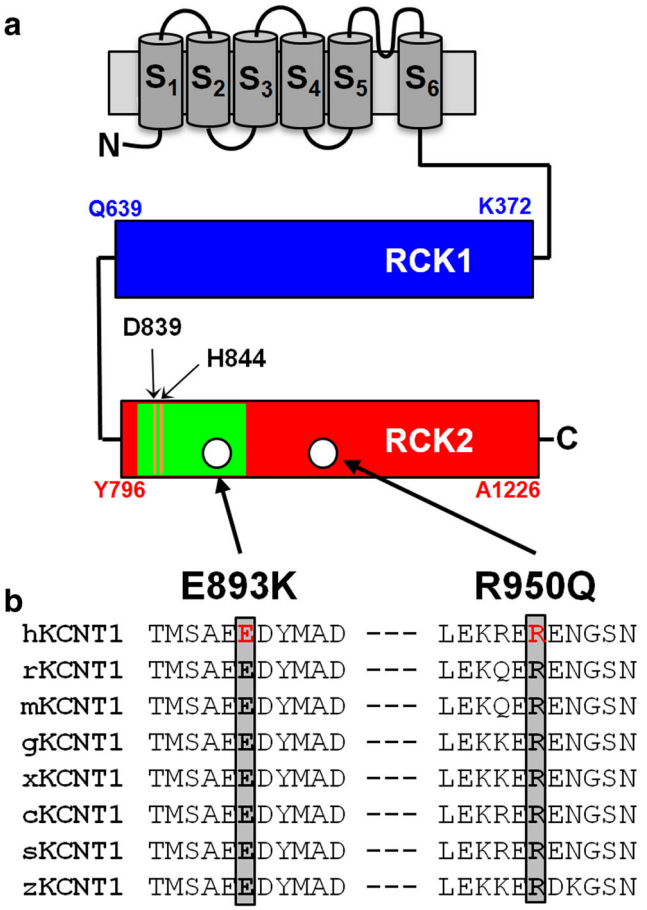

Fig. 5 Topological organization of a KCNT1 subunit and localization of the mutations herein investigated. (**a**) Topological representation of a single KCNT1 subunit. S_1-S_6 indicate transmembrane segments, whereas RCK1 and RCK2 are indicated by blue and red rectangles, respectively. D839 and H844 indicate residues previously shown to confer Na^+-sensitivity to KCNT1 currents [32]. The green box in RCK2 corresponds to the NAD-binding domain. White circles indicate the position of the mutated residues herein investigated. (**b**) Partial alignment of KCNT1 subunits of different species (h = human, r = rat, m = mouse, g = chicken, x = Xenopus laevis, c = cat, s = sheep, z = zebrafish). Mutated residues herein investigated are in red.

current was detected in nontransfected CHO cells (maximal current density at + 60 mV was 1.4 ± 0.6 pA/pF; Fig. 6a and Table 1), transfection with KCNT1 cDNA elicited robust, outwardly rectifying currents (Fig. 6a) in response to depolarizing voltage pulses from − 90 to + 60 mV (Fig. 6a, b, Table 1). KCNT1 currents displayed complex activation kinetics, with an instantaneous, time-independent component (I_{inst}), followed by a slower, time-dependent one ($I_{steady\text{-}state}$-I_{inst}). At + 60 mV, the ratio between currents measured at the beginning (I_{inst}) and at the end ($I_{steady\text{-}state}$ or I_{ss}) of the depolarizing step was 0.25 ± 0.02. Expression of homomeric KCNT1 channels carrying E893K or R950Q mutations also generated outwardly rectifying currents; when compared to wild-type KCNT1 channels, current densities from mutant homomeric KCNT1 channels at + 60 mV were significantly larger (Fig. 6a, b, Table 1). In addition, in both KCNT1 E893K and KCNT1 R950Q mutant channels, the $I_{inst}/I_{steady\text{-}state}$ ratio was increased when compared to KCNT1. Boltzmann analysis of the G/V curves [25] from KCNT1 E893K and KCNT1 R950Q homomeric channels revealed that the activation midpoints ($V_{1/2}$) were significantly shifted in the hyperpolarizing direction when compared to KCNT1, with a concomitant decrease in slope (*k*). Taken together, these results suggest that both KCNT1 mutations lead to strong gain-of-function effects on KCNT1 channels by increasing the maximal current size and shifting the activation threshold toward less depolarized potentials.

Since both the E893K and R950Q variants in KCNT1 affected residues located in the RCK2 domain, a protein region conferring current sensitivity to changes in $[Na^+]_i$ [11, 32], the hypothesis that each mutation interferes with the Na^+-dependent current regulation was also tested. To this aim, patch-clamp recordings were performed in Na^+_i-free conditions. Using Na^+-free intracellular solutions, KCNT1 currents were decreased by a factor of 5 (from 104.1 ± 11.4 to 20.0 ± 2.9 pA/pF); by contrast, the currents carried by KCNT1 E893K or KCNT1 R950Q homomeric channels appeared to be less sensitive to the removal of Na^+_i, showing a reduction of approximately 2-folds (from 229.0 ± 20.3 to 101.0 ± 17.6 pA/pF) or 4-folds (from 231.3 ± 21.1 to 52.3 ± 10.5 pA/pF), respectively ($p < 0.05$ *versus* wild-type KCNT1 channels) (Fig. 6b). As a result, current size in Na^+_i-free solutions was much larger in KCNT1 channels carrying the E893K or R950Q mutations when compared to wild-type KCNT1 channels, suggesting that both mutations (and particularly E893K) facilitated activation gating in the virtual absence of Na^+_i.

To reproduce the genetic status of EIMFS patients, carrying only 1 mutated KCNT1 allele, wild-type and mutant KCNT1 cDNAs were co-transfected in CHO cells at a 0.5:0.5 ratio. As shown in Table 1, current densities from cells expressing KCNT1+KCNT1 E893K or KCNT1+KCNT1 R950Q heteromers were larger than those from KCNT1 homomers. Moreover, currents expressed by KCNT1+KCNT1 E893K or KCNT1+KCNT1 R950Q heteromeric channels showed an intermediate behavior between wild-type and mutant homomeric channels, both in terms of voltage-dependence of activation ($V_{1/2}$, *k*) and in terms of activation kinetics ($I_{inst}/I_{steady\text{-}state}$), suggesting that the extent of mutation-induced gating changes largely depends on the number of mutant subunits incorporated.

Pharmacological modulation of wild-type and mutant KCNT1 channels

The well-known KCNT1 current blocker quinidine (1-1000 μM; Fig. 6c) produced a concentration-dependent decrease in KCNT1 outward currents, with an IC_{50} of 81.1 ± 0.1 μM, as previously reported [17]. Notably, quinidine was even more potent in blocking KCNT1 E893K or KCNT1

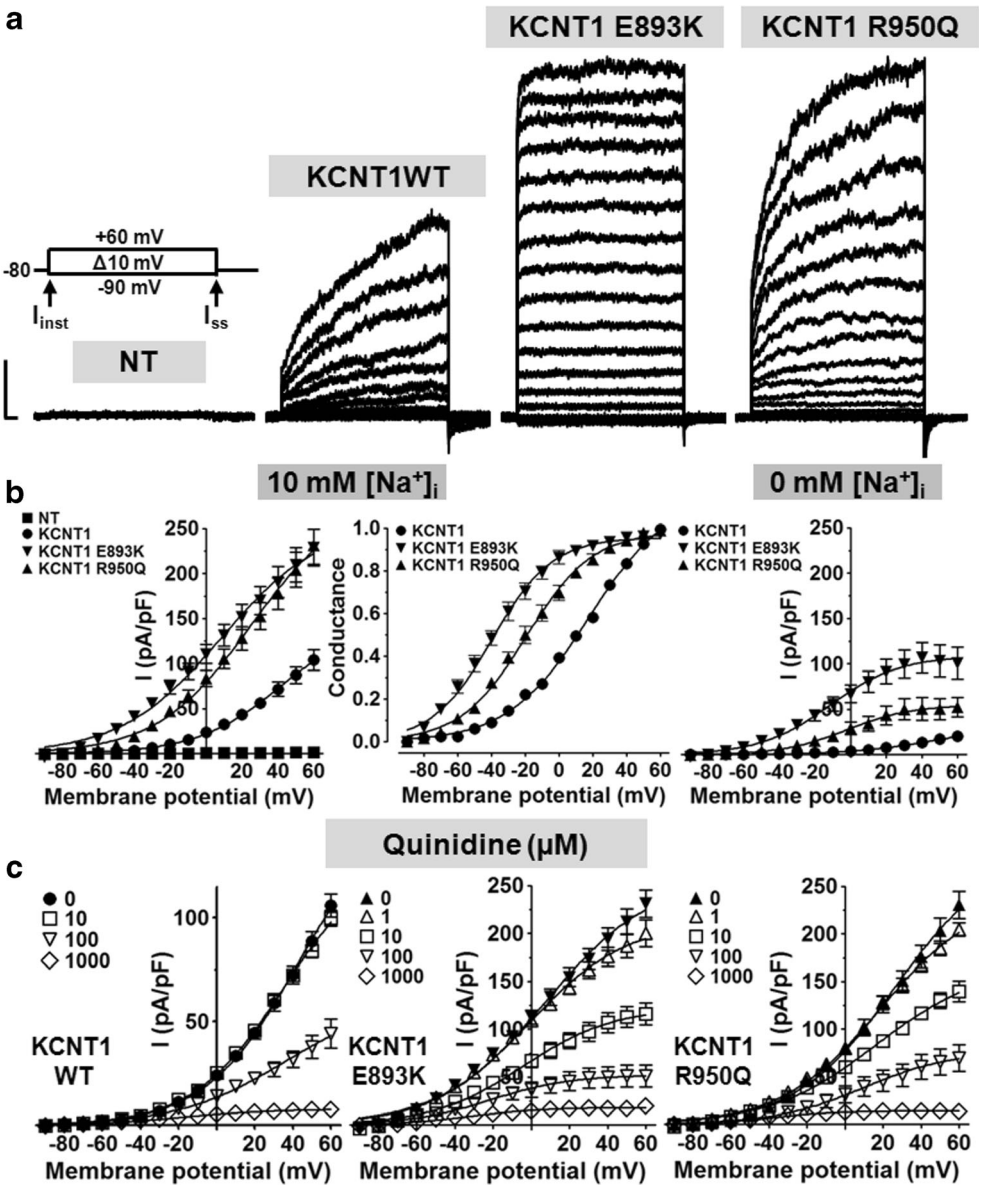

Fig. 6 Functional characterization of wild-type and mutant KCNT1 channels. (**a**) Current traces from CHO cells untransfected (NT) or transfected with expression vectors encoding wild-type or mutant homomeric KCNT1 channels, as indicated, in response to the voltage protocol shown in the inset. The arrows on the voltage protocol indicate the time chosen for current analysis, as explained in the text. (**b**) Current density (left panel) and normalized conductance (middle panel) of wild-type and mutant homomeric KCNT1 channels, as indicated, recorded with 10 mM NaCl in the pipette solution (10 mM Na^+). Right panel: current density of wild-type and mutant KCNT1 channels, recorded without NaCl in the pipette (0 mM Na^+). (**c**) Current densities from CHO cells expressing homomeric wild-type or mutant KCNT1 channels, as indicated, as a function of quinidine concentrations (1-1000 μM).

R950Q channels (the IC_{50}s were 9.6 ± 2.5 μM or 24.0 ± 5.7 μM, respectively; Table 1). At 1 to 10 μM, a concentration range close to the steady-state free plasma drug concentrations associated with anti-convulsant efficacy (2-5 μg/ml) (see below), quinidine failed to affect KCNT1 channels, whereas it caused a significant ~40% blockade of both KCNT1 E893K or KCNT1 R950Q-mediated currents (Fig. 6c). Notably, heteromeric channels formed upon co-expression of KCNT1 and KCNT1 E893K or KCNT1 R950Q mutant subunits displayed a quinidine sensitivity intermediate between wild-type and mutant homomeric channels (Table 1). These results suggest that quinidine could counteract the *in vitro* gain-of-function phenotype shown by KCNT1 E893K or KCNT1 R950Q channels; in addition, the higher blocking potency of the drug on mutant *versus* wild-type KCNT1 currents suggests a preferential activity of the drug on mutant subunits, strongly supporting the potential use of this drug to control seizures in patients with EIMFS associated to *KCNT1* gain-of-function mutations.

Molecular modeling

State-dependent homology modeling using chicken KCNT1 channels determined by cryo-electron microscopy [26] was then used to infer potential mechanism(s) by which the R950 and E893 residues affected by the mutations herein identified might regulate channel opening. Analysis of the 3D model of KCNT1 tetrameric channel revealed that the E893 residue is involved in state-dependent hydrogen bonds with channel residues of a neighboring subunit, and in particular with the N-lobe RCK1, a domain showing wide conformational changes during channel opening, mainly adopting an expanded conformation compared to the close state [26]. In

Table 1 Biophysical and pharmacological properties of wild-type and mutant KCNT1 channels

	Transfected cDNA (μg)	*n*	Current density at + 60 mV (pA/pF)	$V_{½}$ (mV)	*k* (mV/efold)	$I_{inst}/I_{steady\text{-}state}$	Quinidine IC_{50} at + 60 mV (μM)
NT	–	5	1.4 ± 0.6*	ND	ND	ND	ND
KCNT1	3.6	29	104.1 ± 11.4	17.5 ± 2.1	23.9 ± 1.0	0.25 ± 0.02	81.1 ± 0.1
KCNT1 E893K	3.6	21	229.0 ± 20.3*	− 39.7 ± 1.3*	17.9 ± 1.2*	0.81 ± 0.03*	9.6 ± 2.5*
KCNT1 R950Q	3.6	21	231.3 ± 21.2*	− 19.4 ± 1.4*	19.6 ± 1.0*	0.44 ± 0.04*,#	24.0 ± 5.7*,#
KCNT1 + empty vector	1.8 + 1.8	21	109.6 ± 10.7	14.6 ± 1.9	21.7 ± 0.9	0.26 ± 0.02	ND
KCNT1+KCNT1 E893K	1.8 + 1.8	25	165.8 ± 14.0*,#	− 23.2 ± 1.9*,#	21.5 ± 1.2#	0.53 ± 0.03*,#	42.1 ± 2.9*,#
KCNT1+KCNT1 R950Q	1.8 + 1.8	24	156.6 ± 13.6*,§	− 9.7 ± 1.4*,§,†	20.9 ± 0.9*	0.35 ± 0.02*,§,†	55.2 ± 4.1*,§,†

NT = nontransfected CHO cells; ND = not detected.

*$p < 0.05$ *versus KCNT1*.

# $p < 0.05$ *versus KCNT1 E893K*.

§ $p < 0.05$ *versus KCNT1 R950Q*.

† $p < 0.05$ *versus KCNT1+KCNT1 E893K*.

particular, the negatively charged carboxyl group of E893 interacts by a nonclassical hydrogen bond with the S435 residue in the closed state (Fig. 7; top panel), and with a classical hydrogen bond with Q470 in the open state (Fig. 7; bottom panel) [34]. Replacement of the glutamate residue at position 893 with a lysine (E893K) did not affect the interaction with the S435 residue in the closed state, whereas it introduced an unfavorable (charge repulsion) interaction between K893 and Q470 residues in the open state; thus, the E893K substitution appears to mainly affect the open state of the channel, possibly increasing RCK1 N-lobe expansion during channel opening, providing a plausible explanation for the observed gain-of-function phenotype. A similar mechanism, namely changes in electrostatic interactions, may also explain the gain-of-function properties of KCNT1 channels carrying the R950Q disease-causing substitution, although the functional changes appear to be less prominent when compared to the E893K substitution, and structural analysis of the model did not reveal significant state-dependent interactions involving this residue.

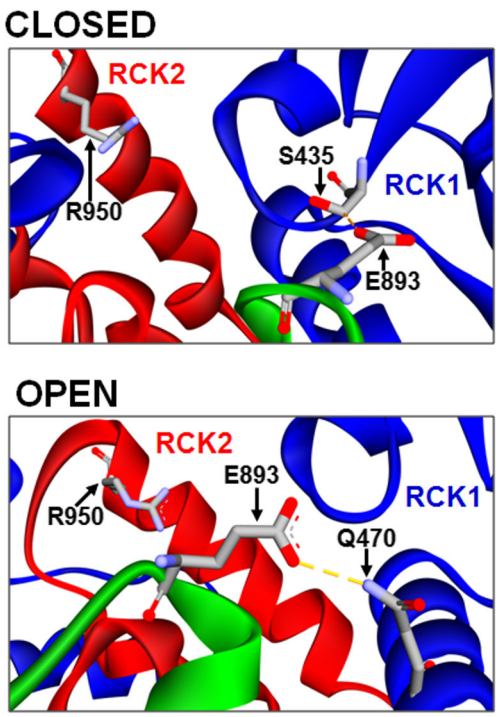

Fig. 7 State-dependent homology modeling of a cytoplasmic region of the KCNT1 subunit. Homology models of the closed (upper panel) and open (lower panel) states of KCNT1 channels. Residues involved in electrostatic interactions are indicated. RCK1 or RCK2 domains are in blue or red, respectively, whereas in green is the NAD-binding region within the RCK2 domain.

DISCUSSION

Personalized treatment in EIMFS

The advent of NGS methods has revolutionized diagnostic procedures in developmental epileptic encephalopathies, allowing an early identification of the specific molecular defects in an ever-growing number of epilepsy-related genes [35]. Early genetic diagnosis is critical for patient stratification and personalized therapy. As an example, in *SCN2A*-related epilepsies, 2 distinct age-dependent phenotypes occurring in the early infantile (< 3 months) or in infantile/childhood (≥ 3 months) periods have been described; whereas the early infantile form responded well to therapy with sodium channel blockers, these drugs were rarely effective or even detrimental in later-onset forms [36].

Despite the phenotypic heterogeneity in terms of age of onset, clinical features, and cognitive outcome, *KCNT1*-related epilepsies are considered paradigmatic examples of epileptic disorders amenable to personalized therapy. In fact, given that the vast majority of epileptogenic *KCNT1* mutations produce an enhancement (gain-of-function) of channel function *in vitro*

[3], and that the KCNT1 blocker quinidine can reverse this *in vitro* phenotype [16], rational, albeit off-label, treatment with quinidine has been attempted in patients affected with mild and severe phenotypes of *KCNT1*-related epilepsies [37]. EIMFS lies on the more critical end of the phenotypic spectrum of *KCNT1*-related epilepsies; it is characterized by focal seizures resistant to conventional anti-epileptic drugs and developmental arrest or regression, severe disability, and high probability of death in the first years of life [1]. Therefore, also considering the poor response to most anti-convulsant treatments, including the ketogenic diet [23], patients with EIFMS often have no therapeutic opportunities alternative to quinidine at the present moment. However, clinical response to quinidine has been quite heterogeneous, with some patients showing good efficacy [18–20], but others in whom lack of efficacy or excessive toxicity has been reported [21–23]. Several interconnected factors, such as the natural history and severity of the underlying disease, the specific molecular defect, the age of symptom onset, and the age at which quinidine therapy was initiated, as well as drug-specific pharmacokinetic and pharmacodynamic factors among others, might provide plausible explanations for such heterogeneity. We believe that the 2 EIMFS cases herein described provide the opportunity to discuss some of these critical factors, in the hope to further optimize treatment opportunities in this devastating developmental encephalopathy. To facilitate data comparison and discussion, Table 2 reports all published cases of *KCNT1*-related epilepsies patients undergoing treatment with quinidine.

Early recognition, genetics, and treatment of EIMFS in 2 novel cases

In our patients, the diagnosis of EIMFS was based on neonatal-onset seizures with autonomic features and focal ictal theta-apha rhythmical EEG activity. Despite aggressive treatment, seizure number gradually increased, with the occurrence of epileptic spasms or myoclonias and malignant migrating focal seizures in few days or weeks after birth. Semiological suspicion prompted genetic investigations, revealing the occurrence of 2 different heterozygous *de novo* variants in *KCNT1*: R950Q in patient 1 and E893K in patient 2. The first variant was previously reported in other EIMFS-affected patients [6, 31], as well as in patients with nocturnal frontal lobe epilepsy (NFLE) [29], mild intellectual disability, psychomotor retardation, and psychiatric symptoms (psychosis, depression, inertia) [30], confirming phenotypic heterogeneity in *KCNT1*-related epilepsies [10]; instead, the E893K variant found in patient 2 is novel.

Electrophysiological assays *in vitro* revealed that both mutations produced a gain-of-function effect on KCNT1 currents; these results are largely consistent with the reported effects of disease-causing *KCNT1* mutations [3, 17]. More importantly, our results clearly demonstrated that, when compared to wild-type KCNT1, mutant channels were more potently blocked by quinidine. In cardiac voltage-gated K^+ channels, quinidine blocks the pore from the inside of the membrane once the activation gate opens by an open-channel blocking mechanism [39]; thus, it seems possible to speculate that mutations increasing the opening probabilities of the channels such as those herein investigated may favor the interaction with quinidine, thus leading to the observed increase in drug's apparent affinity [40]. Based on this preclinical evidence and given the dramatic trend to progressive seizure increase and of refractoriness to multiple conventional anti-convulsants, quinidine therapy was started at 3.5 months of age in patient 1 and at 16 months of age in patient 2. Together with another recently reported EIMFS patient with focal seizure onset at 3 days of age who also started quinidine therapy at 3 months of age (patient 2 in [38]), patient 1 is the youngest EIMFS child being treated with quinidine. In both our patients, following treatment with quinidine, we observed a reduction of seizure frequency by > 90%. Although the clinical-instrumental improvement observed over time might reflect the natural history of EIFMS, the temporal correlation between quinidine treatment with the amelioration of EEG pattern and seizure burden in both patients allows to hypothesize that the improvement is attributable to this specific pharmacological treatment, and cannot be accounted for by the marked fluctuations in seizure number spontaneously occurring during the disease course. These observations are further supported by the temporal association between reduced quinidine plasma levels and seizure recurrence, even if seizures were never fully controlled despite optimal quinidine levels. Moreover, case 2 is actually in monotherapy with quinidine with good control of seizures, further supporting the correlation between this specific drug and the clinical-instrumental positive response. Overall, the present results are in line with the hypothesis that therapeutic response might be age-dependent, with all patients initiating treatment below age 4 years being responsive, whereas those undergoing quinidine therapy after 4 years being, instead, nonresponsive [38].

However, even if we observed a significant effect on seizure control and EEG features following quinidine treatment, the severe cognitive and motor disability appears only marginally affected by this therapy. Despite the young age of treatment initiation, it seems possible to hypothesize that the "therapeutic window" for intervention is even more anticipated because of a critical developmental role played by KCNT1 channels. In fact, in mice, KCNT1 transcripts are detected at similar levels throughout the brain at birth, showing a marked increase during the first 2 weeks of life in cortex and cerebellum, without concomitant changes in the hippocampus and thalamus [16]. In addition, KCNT1 channels directly interact with the fragile X mental retardation protein (FMRP), whose deletion is the most common cause for intellectual disability and inherited autism, and IK_{Na} is reduced in animal models of fragile X syndrome that lack FMRP [41]. Therefore, patients may have irreversible brain dysfunction prior to initiation of therapy due to aberrant

Table 2 Quinidine treatment in patients with *KCNT1* mutations

#	*KCNT1* mutation	Seizure type	Age of seizure onset	Age of beginning of quinidine therapy	Clinical response to quinidine	Maximal quinidine dose (mg/kg/day)	Additional drugs	Serum levels of quinidine (μg/ml)	QT prolongation	*In vitro* studies	*In vitro* response to quinidine	References
1	c.1283G>A; p.R428Q	EIMFS	10 weeks	2 years	Complete seizure control; improved psychomotor devolopment	42	Topiramate, levetiracetam, clobazam, gabapentin, ketogenic diet ineffective or poorly effective	2.0-4.0	No	GOF	Yes (less effective than W-T)	[16, 18]
2	c.2386T>C; p.Y796H	Nocturnal focal seizures	18 months	11 years	No	54.2	12 anti-epileptic medications and the ketogenic diet had failed	1.7	Yes	GOF	Yes	Patient 1 in [20]; [16]; same mutation in a patient with ADNFLE [4]
3	c.1887G>C; p.K629N	EIMFS	4 months	3 years	80% seizure reduction	34.4	8 anti-epileptic medications and the ketogenic diet had failed	0.77	No	GOF	Yes (less effective than WT)	Patient 2 in [20]
4	c.1283G>A; p.R428Q	EIMFS	6 weeks	5 years	No	73	Multiple anti-epileptic drugs had failed; partial response to vagal nerve stimulation and ketogenic diet	1.5-3	ND	GOF	Yes (less effective than WT)	[16, 21]; same mutation also found in a patient with EOEE (patient 11 in [7])
5	c.1955G>T; p.G652V	West syndrome	5 months	2.5 years	Yes, reduction in epileptic spasms, decreased paroxysmal activity	60	VPA, vit. B6, zonisamide, topiramate, nitrazepam, lamotrigine, ketogenic diet, all poorly effective	2.7-4.8	Yes	ND	ND	[19]
6	c.1421G>A; p.R474H	Asymmetric tonic seizures	1 week	9 years	None	37-45	6 anti-epileptic drugs, vagal nerve stimulation and ketogenic diet had failed	1.1 (at 37); 2.6 (at 45)	Yes	ND	ND	Patient 1 in [38]
7	c.2965G>T; p.?	Focal seizures	3 days	3 months	Yes, seizure reduction	40	8 anti-epileptic drugs and ketogenic diet had failed	0.4	Yes	ND	ND	Patient 2 in [38]
8	c.1193G>A; p.R398Q	Focal seizures	4 years	> 4 years	None	60	Seizures were refractory to 3 (unknown) antiepileptics	0.4-3.2	Yes	GOF	Yes	Patient 3 in [39]; patient 2 in [6]; [16]
9	c.820C>A; p.L274I	EIMFS	1 day	ND	None	40	At least 5 different drugs had failed	ND	No	GOF	Yes (less effective than WT)	Patient 2 in [31]
10	c.1504T>G; p.F502V	EIMFS	3 months	ND	Yes, seizure reduction	40	At least 5 different drugs had failed	ND	ND	GOF	Yes	Patient 5 in [38]
11	c.2687T>A; p.M896K	EIMFS	2 weeks	ND	None	30	At least 5 different drugs had failed	ND	ND	GOF	Yes	Patient 6 in [38]
12	c.2782C>T; p.R928C	ADNFLE	2-15 years	> 15 years	None	300 mg/day	Before quinidine, many and distinct AEDs for each patient; 2 patients also used phenytoin during quinidine treatment	< 0.21	No (in patients completing the trial)	GOF	Yes	[6, 16, 29]
13	c.2849G>A; p.R950Q	ADNFLE	2-15 years	> 15 years	None	300 mg/day	Before quinidine, many and distinct AEDs for each patient; 2 patients	< 0.21	No (in patients	GOF	Yes	[6, 29–31]

Table 2 (continued)

#	*KCNT1* mutation	Seizure type	Age of seizure onset	Age of beginning of quinidine therapy	Clinical response to quinidine	Maximal quinidine dose (mg/kg/day)	Additional drugs	Serum levels of quinidine (μg/ml)	QT prolongation	*In vitro* studies	*In vitro* response to quinidine	References
							also used phenytoin during quinidine treatment		completing the trial)			
14	c.808C>G; p.Q270E	EIMFS	3 days	6 months	None; died at 9 months	35	Failed multiple AED trials, at maximal doses	ND	Yes	ND	ND	[22]
15	c.2849G>A; p.R950Q	EIMFS	2 days	3.5 months	Yes; 90% seizure frequency reduction	45	Failed previous treatments with several anti-convulsants	2.7	Yes	GOF	Yes (more effective than WT)	Present study
16	c.2677G>A; p.E893K	EIMFS	1 day	16 months	Yes; 90% seizure frequency reduction	58	Failed previous treatments with several anti-convulsants	3.5	No	GOF	Yes (more effective than WT)	Present study

neurodevelopment, possibly already *in utero*, and earlier initiation of quinidine, such as at onset of epilepsy, might have positively influenced cognitive progression. On the other hand, therapy initiation at a developmental stage when permanent epileptogenic brain injury has occurred may explain poor responses to quinidine [21].

Genotype-phenotype correlations

Analysis of the reported cases of patients carrying KCNT1 mutations being treated with quinidine, as also summarized in Table 2, reveals a high variability in terms of, among other factors, variant type, genetic transmission (sporadic EIMFS *versus* autosomal-dominant nocturnal frontal lobe epilepsy or ADNFLE), age of seizures onset, age of beginning of quinidine treatment, and quinidine blood levels; thus, it seems premature to draw specific conclusions on how each of these factors influences quinidine efficacy. The role of the specific variant is possibly highlighted by the EIMFS patient 2 reported by McTague et al. [31]; in fact, this patient, despite being diagnosed (and possibly treated) very early, received a similar dosage of quinidine (40 mg/kg/day) to the patients herein reported, but did not respond to quinidine, possibly because channels formed by subunits carrying the L274I pore variant found in this patient displayed a significant reduction in quinidine sensitivity *in vitro* when compared to wild-type channels [31]. Along the same line, patient 4 in the same report [31], who carried the F346L variant, was not treated with quinidine because of the observed *in vitro* insensitivity to the drug of KCNT1 channels carrying this variant. On the other hand, patients carrying the R428Q mutation, another gain-of-function variant slightly reducing quinidine sensitivity *in vitro* [16], have been reported to show heterogeneous clinical responses to quinidine: in fact, whereas the patient of Bearden et al. [18] was successfully treated with quinidine at 2 years of age, that one of Chong et al. [21] failed to respond to the drug when treatment was initiated at 5 years of age. Therefore, these data, although anecdotal and limited to single patient cases, further support that early treatment with quinidine is critical for anti-epileptic efficacy.

Pharmacokinetics and pharmacodynamics of quinidine: Critical issues and correlation between *in vitro* and *in vivo* data

In addition to preclinical evidence showing gain-of-function consequences prompted by the specific variant, availability of adequate resources for therapeutic drug monitoring appears as a necessary prerequisite for quinidine therapy optimization. As herein shown, quinidine is often prescribed in association with drugs inducing quinidine metabolism (like carbamazepine or phenobarbital), or decreasing quinidine blood levels and causing rebound increases (such as upon withdrawal of the ketogenic diet or of topiramate). In our experience, plasma levels rather

than daily doses are more faithful predictors of clinical responses; stable responses in our patients were observed at plasma levels between 2.7 and 3.5 μg/ml, well within the conventional range for anti-arrhythmic efficacy (2-5 μg/ml), and seizure relapsed when quinidine levels fell below 2 μg/ml. Suboptimal drug plasma levels might have contributed, in one with other factors, to the recently reported lack of response of oral quinidine in adult patients with severe ADNFLE due to *KCNT1* mutation (Table 2) [29]. Noteworthy, careful evaluation of blood quinidine levels appears mandatory also to minimize drug-induced cardiac toxicity; abnormal QT interval values (up to 505 ms in our patient 1) were observed in coincidence with increases in quinidine levels, particularly at the earliest stages of therapy, even at plasma levels below 2 μg/ml. Thus, as reported previously [29], quinidine titration was initially limited by abnormal QT values, with QT increase and seizure reduction often appearing as tightly linked to abrupt changes in quinidine plasma levels. The existing correlation between quinidine plasma levels, QT intervals, and seizure frequency is problematic, as it clearly decreases the drug therapeutic index. A collaborative multidisciplinary team including pediatric epileptologists, cardiologists, and intensive care monitoring services is needed to disentangle such deleterious correlation and optimize risk/benefit ratios of quinidine therapy, in order to achieve drug plasma levels avoiding both the deleterious developmental effects of status epilepticus and the potentially-fatal risks of cardiac complications. Additional concerns, also herein highlighted, relate to co-treatment with levetiracetam, which may further increase the QT interval in at-risk patients [42].

Quinidine is not a potent antagonist of KCNT1 channels and has relatively scarce blood–brain barrier penetration; its brain concentrations during standard therapy are unknown, although it has been suggested that they may be lower than those needed to normalize pathological KCNT1 conductance [18]. The therapeutic range for quinidine (2-5 μg/ml) corresponds to a steady-state free plasma drug levels of ~1 to 8 μM, when considering an unbound fraction of 15 to 40% (depending on drug concentration) [43]; notably, in our *in vitro* experiments, 10 μM quinidine was significantly more effective in blocking mutant channels when compared to wild-type channels, thus suggesting that the drug concentrations used *in vitro* might fall within a clinically relevant range, and that significant target engagement may occur *in vivo*. Quinidine brain levels are limited by the drug's ability to act as a substrate for ABCB1/P-glycoprotein (P-gp)/MDR1 transporters at the blood–brain barrier [44]; therefore, it seems likely that additional KCNT1 blockers with improved brain penetration may at least partially overcome some of the pharmacodynamic and pharmacokinetic limitations shown by quinidine. Finally, the 2 variants found in our patients fall within the RCK2 domain, a protein region conferring strong current sensitivity to changes in $[Na^+]_i$ [11, 33]; *in vitro*, R950Q or E893K mutant channels appear rather insensitive to changes in $[Na^+]_i$ as they carry a substantial amount of currents even in the absence of intracellular $[Na^+]_i$. This result may provide a plausible explanation for the lack of anti-convulsant efficacy observed in our patients (and for most EIMFS patients) to classical Na^+ channel blockers.

CONCLUSIONS

We describe clinical, genetic, and *in vitro* preclinical data on 2 patients with *KCNT1*-related EIMFS, focusing on some of the critical issues of personalized therapy with quinidine. Despite the present overexpression cellular model may overstate the functional effect of the mutations and could not recapitulate time- and region-dependent changes in brain expression of specific variants, the present data highlight the critical prognostic role of preclinical tests shedding light on the specific, mutation-dependent changes in channel function and pharmacological sensitivity for optimal personalized treatment of EIMFS patients. Also, our results show the extreme difficulties when managing such delicate and complex cases, pinpointing to the need for well-defined titration and monitoring protocols shared by multidisciplinary teams. Multicentre studies in genetically characterized and age-stratified populations of EIMFS patients are urgently needed to find an optimal balance between drug efficacy on seizure frequency and, possibly, developmental outcomes, and its complex safety profile.

Acknowledgments The present work was supported by the Telethon Foundation (grant number GGP15113) to MT, the Italian Ministry of Health Ricerca Finalizzata Giovani Ricercatori 2010 (Project GR-2010-2304834 to JCD) and Ricerca Finalizzata Giovani Ricercatori 2016 (Project GR-2016-2363337 to JCD and MVS), and the Italian Ministry for University and Research (Project Scientific Independence of Researchers 2014 RBSI1444EM) and the University of Naples "Federico II" and Compagnia di San Paolo in the frame of Program STAR "Sostegno Territoriale alle Attività di Ricerca" (project number 6-CSP-UNINA-120) to FM.

Required Author Forms Disclosure forms provided by the authors are available with the online version of this article.

References

1. Coppola G, Plouin P, Chiron C, Robain O, Dulac O. Migrating partial seizures in infancy: a malignant disorder with developmental arrest. Epilepsia 1995;36:1017–1024.
2. Striano P, Coppola G, Zara F, Nabbout R. Genetic heterogeneity in malignant migrating partial seizures of infancy. Ann Neurol 2014;75:324–326.
3. Barcia G, Fleming MR, Deligniere A, et al. De novo gain-of-function KCNT1 channel mutations cause malignant migrating partial seizures of infancy. Nat Genet 2012;44:1255–1259.
4. Heron SE, Smith KR, Bahlo M, et al. Missense mutations in the sodium-gated potassium channel gene KCNT1 cause severe autosomal dominant nocturnal frontal lobe epilepsy. Nat Genet 2012;44:1188–1190.
5. Martin HC, Kim GE, Pagnamenta AT, et al. Clinical whole-genome sequencing in severe early-onset epilepsy reveals new genes and

improves molecular diagnosis. Hum Mol Genet 2014;23:3200–3211.
6. Møller RS, Heron SE, Larsen LH, et al. Mutations in KCNT1 cause a spectrum of focal epilepsies. Epilepsia 2015;56:e114-e120.
7. Ohba C, Kato M, Takahashi N, et al. De novo KCNT1 mutations in early-onset epileptic encephalopathy. Epilepsia 2015;56:e121-e128.
8. Juang JM, Lu TP, Lai LC, et al. Disease-targeted sequencing of ion channel genes identifies de novo mutations in patients with non-familial Brugada syndrome. Sci Rep 2014;4:6733.
9. Hansen N, Widman G, Hattingen E, Elger CE, Kunz WS. Mesial temporal lobe epilepsy associated with KCNT1 mutation. Seizure 2017;45:181–183.
10. Lim CX, Ricos MG, Dibbens LM, Heron SE. KCNT1 mutations in seizure disorders: the phenotypic spectrum and functional effects. J Med Genet 2016;53:217–225.
11. Yuan A, Santi CM, Wei A, et al. The sodium-activated potassium channel is encoded by a member of the Slo gene family. Neuron 2003;37:765–773.
12. Bhattacharjee A, Joiner WJ, Wu M, Yang Y, Sigworth FJ, Kaczmarek LK. Slick (Slo2.1), a rapidly-gating sodium-activated potassium channel inhibited by ATP. J Neurosci 2003; 23:11681–11691.
13. Franceschetti S, Lavazza T, Curia G, et al. Na^+-activated K^+ current contributes to postexcitatory hyperpolarization in neocortical intrinsically bursting neurons. J Neurophysiol 2003;89:2101–2111.
14. Martinez-Espinosa PL, Wu J, Yang C, et al. Knockout of Slo2.2 enhances itch, abolishes KNa current, and increases action potential firing frequency in DRG neurons. Elife 2015;4. pii: e10013.
15. Evely KM, Pryce KD, Bausch AE, et al. Slack K_{Na} Channels Influence Dorsal Horn Synapses and Nociceptive Behavior. Mol Pain 2017;13:1744806917714342.
16. Milligan CJ, Li M, Gazina EV, et al. KCNT1 gain of function in 2 epilepsy phenotypes is reversed by quinidine. Ann Neurol 2014;75:581–590.
17. Rizzo F, Ambrosino P, Guacci A, et al. Characterization of two de novo KCNT1 mutations in children with malignant migrating partial seizures in infancy. Mol Cell Neurosci 2016;72:54–63.
18. Bearden D, Strong A, Ehnot J, DiGiovine M, Dlugos D, Goldberg EM. Targeted treatment of migrating partial seizures of infancy with quinidine. Ann Neurol 2014;76:457–461.
19. Fukuoka M, Kuki I, Kawawaki H, et al. Quinidine therapy for West syndrome with KCNTI mutation: A case report. Brain Dev 2017;39:80–83.
20. Mikati MA, Jiang YH, Carboni M, et al. Quinidine in the treatment of KCNT1-positive epilepsies. Ann Neurol 2015;78(6):995–999.
21. Chong PF, Nakamura R, Saitsu H, Matsumoto N, Kira R. Ineffective quinidine therapy in early onset epileptic encephalopathy with KCNT1 mutation. Ann Neurol 2016;79:502–503.
22. Madaan P, Jauhari P, Gupta A, Chakrabarty B, Gulati S. A quinidine non responsive novel KCNT1mutation in an Indian infant with epilepsy of infancy with migrating focal seizures. Brain Dev 2017;40:229–232.
23. Mori T, Imai K, Oboshi T, et al. Usefulness of ketogenic diet in a girl with migrating partial seizures in infancy. Brain Dev 2016;38:601–604.
24. Ambrosino P, Soldovieri MV, De Maria M, Russo C, Taglialatela M. Functional and biochemical interaction between PPARalpha receptors and TRPV1 channels: potential role in PPARalpha agonists-mediated analgesia. Pharmacol Res 2014;87:113–122.
25. Miceli F, Soldovieri MV, Ambrosino P, et al. Early-onset epileptic encephalopathy caused by gain-of-function mutations in the voltage sensor of Kv7.2 and Kv7.3 potassium channel subunits. J. Neurosci 2015;35:3782–3793.
26. Hite RK, MacKinnon R. Structural Titration of Slo2.2, a Na^+-Dependent K^+ Channel. Cell 2017;168:390–399.
27. Schwede, T., Kopp, J., Guex, N. & Peitsch, M. C. SWISS-MODEL: An automated protein homology-modeling server. Nucleic Acids Res. 2003; 31:3381–3385.
28. Soldovieri MV, Ambrosino P, Mosca I, et al. Early-onset epileptic encephalopathy caused by a reduced sensitivity of Kv7.2 potassium channels to phosphatidylinositol 4,5-bisphosphate. Sci Rep 2016;6:38167.
29. Mullen SA, Carney PW, Roten A, et al. Precision therapy for epilepsy due to KCNT1 mutations: A randomized trial of oral quinidine. Neurology 2018;90:e67-e72.
30. Hildebrand MS, Myers CT, Carvill GL, et al. A targeted resequencing gene panel for focal epilepsy. Neurology 2016;86:1605–1612.
31. McTague A, Nair U, Malhotra S, et al. Clinical and molecular characterization of KCNT1-related severe early-onset epilepsy. Neurology 2018;90:e55-e66.
32. Zhang Z, Rosenhouse-Dantsker A, Tang QY, Noskov S, Logothetis DE. The RCK2 domain uses a coordination site present in Kir channels to confer sodium sensitivity to Slo2.2 channels. J Neurosci 2010;30:7554–7562.
33. Tamsett TJ, Picchione KE, Bhattacharjee A. NAD^+ activates K_{Na} channels in dorsal root ganglion neurons. J Neurosci 2009;29:5127–5134.
34. Pierce AC, Sandretto KL, Bemis GW. Kinase inhibitors and the case for CH…O hydrogen bonds in protein-ligand binding. Proteins 2002;49:567–576.
35. Moller RS, Dahl HA, Helbig I. The contribution of next generation sequencing to epilepsy genetics. Expert Rev Mol Diagn 2015;15:1531–1538.
36. Wolff M, Johannesen KM, Hedrich UB, et al. Genetic and phenotypic heterogeneity suggest therapeutic implications in SCN2A-related disorders. Brain 2017;140:1316–1336.
37. Poduri A. A channel for precision diagnosis and treatment in genetic epilepsy. Ann Neurol 2014;76:323–324.
38. Abdelnour E, Gallentine W, McDonald M, Sachdev M, Jiang YH, Mikati MA. Does age affect response to quinidine in patients with KCNT1 mutations? Report of three new cases and review of the literature. Seizure 2018;55:1–3.
39. Clark RB, Sanchez-Chapula J, Salinas-Stefanon E, Duff HJ, Giles WR. Quinidine-induced open channel block of K^+ current in rat ventricle. Br J Pharmacol 1995; 115:335–343.
40. Yang B, Gribkoff VK, Pan J, et al. Pharmacological activation and inhibition of Slack (Slo2.2) channels. Neuropharmacology 2006;51:896–906.
41. Kim GE, Kaczmarek LK. Emerging role of the KCNT1 Slack channel in intellectual disability. Front Cell Neurosci 2014;8:209.
42. Issa NP, Fisher WG, Narayanan JT. QT interval prolongation in a patient with LQT2 on levetiracetam. Seizure 2015;29:134–136.
43. Harashima H, Sawada Y, Sugiyama Y, Iga T, Hanano M. Analysis of nonlinear tissue distribution of quinidine in rats by physiologically based pharmacokinetics. J Pharmacokinet Biopharm 1985;13:425–440.
44. Sziráki I, Erdo F, Beéry E, et al. Quinidine as an ABCB1 probe for testing drug interactions at the blood-brain barrier: an in vitro in vivo correlation study. J Biomol Screen 2011;16:886–894.